Materials Letters 64 (2010) 2230–2232

Contents lists available at ScienceDirect

Materials Letters

journal homepage: www.elsevier.com/locate/matlet

Ultra-elastic and inelastic impact of Cu nanoparticles

L.B. Han [a,d], Q. An [b,c], S.N. Luo [b,*], W.A. Goddard III [c]

[a] School of Earth and Space Sciences, University of Science and Technology of China, Hefei, Anhui, 230026, PR China
[b] Los Alamos National Laboratory, Los Alamos, NM 87545, USA
[c] Materials and Process Simulation Center, California Institute of Technology, Pasadena, CA 91125, USA
[d] Institute of Geophysics, China Earthquake Administration, Beijing, 100081, PR China

ARTICLE INFO

Article history:
Received 10 June 2010
Accepted 4 July 2010
Available online 15 July 2010

Keywords:
Nanoparticles
Ultra-elastic
Inelastic
Molecular dynamics
Impact

ABSTRACT

The degree of elasticity for the impact of a particle with a rigid wall is normally characterized with the restitution parameter, *R*. We examine such impact behavior of Cu nanoparticles with molecular dynamics simulations, for different particle sizes (1–15 nm in radius) and impact velocities (25–200 m s^{-1}). The impact can be ultra-elastic ($R>1$) or inelastic ($R<1$). Ultra-elastic or inelastic impact may occur for the smallest nanoparticles soly due to fluctuations, and the impact is inelastic but can be highly elastic ($R\sim0.9$–1) for larger sizes. *R* decreases with increasing size and impact velocity in general. Impact-induced structure transitions (e.g., dislocations) can be reversible and induce irreversible heating regardless of their reversibility. Such heating along with remnant plasticity is the key mechanism for impact inelasticity. Inelastic impact may occur with little remnant plasticity.

1. Introduction

The impact of nanoparticles is of interest not only in impact physics [1,2] (e.g., the scaling laws for size and velocity), but also for such applications as coating, materials synthesis, nanotechnology and planet formation. Considerable experimental, theoretical and modeling efforts have been dedicated to particle impact at different scales [2–10], and the literature can hardly be exhausted here. For instances, nanoparticle impact was modeled with molecular dynamics (MD) on the Lennard-Jones system [5,9], Si [6], ice [8] and Au [10], and experiments were conducted on ice particles [7], to investigate impact elasticity or inelasticity, coalescence and fragmentation. Nonetheless, MD simulations of nanoparticle impact still remain underexplored and are largely limited to extremely small nanoparticles and a few substances, and further studies are highly desirable for revealing novel impact phenomena and underlying physics. Impact of a particle with a rigid wall is normally characterized with the restitution parameter *R* [2]. $R>1$, $R=1$, and $R<1$ represent ultra-elastic, perfectly elastic and inelastic impact, respectively. Here we utilize MD to simulate such impact behavior of a representative metallic system (Cu). We examine the impact elasticity of Cu nanoparticles and its dependence on particle size and impact velocity, as well as the related structure features. It is found that the impact of nanoparticles of Cu, one of the most ductile metals, can be ultra-elastic or exceptionally elastic.

2. Methodology

We adopt an accurate embedded-atom-method potential [11] to simulate the impact of Cu nanoparticles on a rigid wall. The spherical nanoparticles are carved out of single crystal Cu, and the radii (r) explored here are 1, 2, 5, 10 and 15 nm, corresponding to system sizes of 369, 2899, 44,115, 354,607 and 1,197,215 atoms, respectively. Each nanoparticle is equilibrated at ambient conditions, and then assigned an impact velocity of v_i along [100] (the *x*-axis) prior to its impact onto a rigid wall (the particle–rigid-wall geometry [8,12]). The *y*- and *z*-axes are along [010] and [001], respectively. No periodic boundary conditions are applied. MD simulations are performed with a microcanonical ensemble. The time step for integrating the equation of motion is 1 fs. MD simulations yield the histories of atomic position, velocity, temperature (T), stress (σ_{ij}; $i,j=x,y$ and z), density and structure properties such as radial distribution function (RDF). Local and bulk average properties can be obtained via averaging in selected regions.

We characterize the impact-induced structural changes with the Honeycutt–Andersen technique [13] in terms of face-centered cubic (fcc), hexagonal closed pack (hcp) and non-close-packed structures. Atoms in the hcp packing are related to stacking faults (and twins), and the non-close-packed atoms, to surfaces, dislocation cores and other defects induced by impact (excluding surface defects). The structure transitions (e.g., stacking fault-related dislocations) may be reversible during unloading. It is well known that the fcc–hcp structure change (and related other defects) is directly related to crystal plasticity in fcc metals. To avoid confusion, plasticity only refers to remnant structure changes after unloading in our discussion below. The nearest-neighbor distance for the Honeycutt–Andersen

* Corresponding author.
E-mail address: sluo@lanl.gov (S.N. Luo).

0167-577X/$ – see front matter © 2010 Elsevier B.V. All rights reserved.
doi:10.1016/j.matlet.2010.07.015

analysis is the first minimum in RDF calculated at a given instant. A similar method of central symmetry [14] is also applied for the structural analysis.

3. Result and discussion

Upon impact (initially point contact), non-planar compressional stress waves propagate into the nanoparticle and are then reflected from the free surface. It remains in contact with the rigid wall and separates at a delay of Δt_{sp} due to unloading, rebounding with a terminal velocity v_t. Here the velocity of a nanoparticle refers to its center of mass velocity, v_c. v_i ranges from 0.025 to 0.2 km s^{-1}, and v_c is obtained as a function of time t (Fig. 1(a)). v_c reaches v_t upon separation and it remains a constant at simulation time scales. The velocity restitution, $R \equiv v_t/v_i$, characterizes the degree of impact elasticity. Figs. 2(a) and 3 present R as a function of particle size and impact velocity.

For the smallest size ($r = 1$ nm), pronounced fluctuations in R occur for a given v_i (Fig. 2(a)). For example, R varies from 0.57 to 1.13 for ten independent runs at $v_i = 0.025$ km s^{-1}. Ultra-elastic impact ($R > 1$) is observed up to ~0.075 km s^{-1}, and its probability appears to decrease with increasing v_i. (The probability for ultra-elastic impact is about 20% for 50 runs. Since the uncertainties are negligible in v_i and v_t (thus R), the observation of such events is of high confidence. However, a full statistics remains to be investigated in the future with a large number of runs.) This ultra-elastic impact was observed for the Lennard-Jones system, and attributed to the marked fluctuations inherent in such small systems [5]. Fluctuations exist in potential and kinetic energies as well as shape, and may induce the conversion of a small portion of the internal energy (Fig. 2(b); also see below) into v_c during the contact period. However, the exact mechanism is still unclear, and possible candidates include the vibration modes of the nanosphere [5]. Ultra-elastic impact is observed for both metallic and molecular systems. By the same token, fluctuations also induce inelastic impact even in the absence of dislocations (see below). With increasing r, the fluctuation in R decreases appreciably: it is noticeable for $r = 2$ nm, but is much smaller and thus neglected for $r \geq 5$ nm. The crossover between these two sizes (2 nm and 5 nm) around v_i ~ 0.075–0.1 km s^{-1} (Fig. 3) is largely caused by the fluctuations for $r = 2$ nm (fluctuations not shown for clarity).

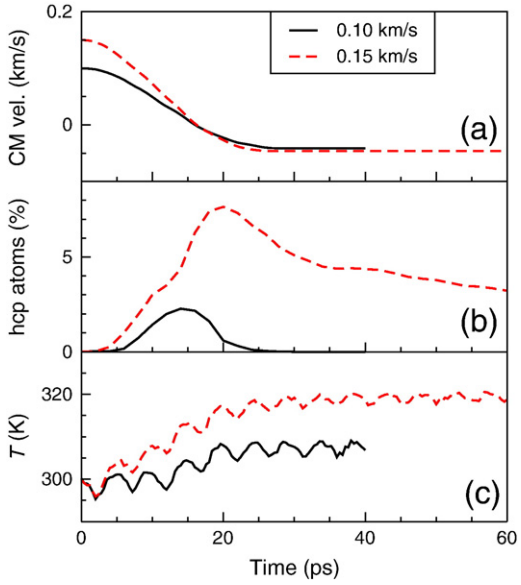

Fig. 1. Evolutions of the center of mass (CM) velocity (a), the percentage of hcp atoms (b) and temperature (c) for the nanoparticles ($r = 10$ nm) at two impact velocities.

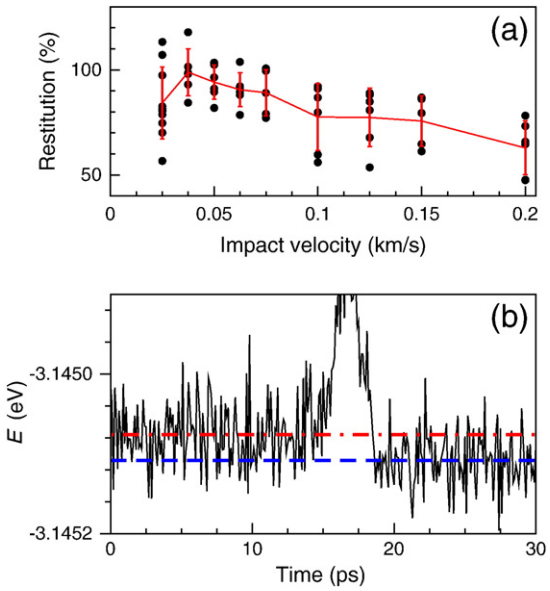

Fig. 2. Impact of small nanoparticles with $r = 1$ nm: (a) velocity restitution vs. impact velocity. Circles denote individual runs, and solid line, their respective averages. (b) Internal energy (E) evolution for an ultra-elastic impact ($v_i = 0.025$ km s^{-1} and $R \approx 1.07$). The dot-dashed and dashed lines denote the averages before and after impact, respectively.

At low impact velocities, there exists approximately a plateau in R (about 0.9–1), i.e., the impact is highly elastic in this regime. It then decreases sharply with increasing v_i due to drastic increase in plastic deformation (see below); this transition occurs at about 0.088, 0.05 and <0.025 km s^{-1} for $r = 5$, 10 and 15 nm with weak fluctuations, respectively, and roughly at 0.075–0.1 km s^{-1} for $r = 1$ and 2 nm. The reduction in R is slowed down at higher impact velocities likely because of plasticity saturation. However, R is still impressive, e.g., it is about 0.3 for $r = 15$ nm and $v_i = 0.15$ km s^{-1}. It is expected that R and its transition velocity decrease at larger particle sizes.

Next we examine impact-induced structural changes (e.g., stacking faults) to make connections with R. Some examples are shown in Figs. 1(b) and 3 inset. (Visualization adopts AtomEye [15].) The onset of the fcc–hcp structure change during impact occurs at v_i ~ 0.15, 0.075, 0.05, 0.025 and 0.025 km s^{-1} for $r = 1$, 2, 5, 10 and 15 nm, respectively. The numbers of the hcp and non-close-packed atoms are nearly zero or insignificant in the plateau regime (roughly

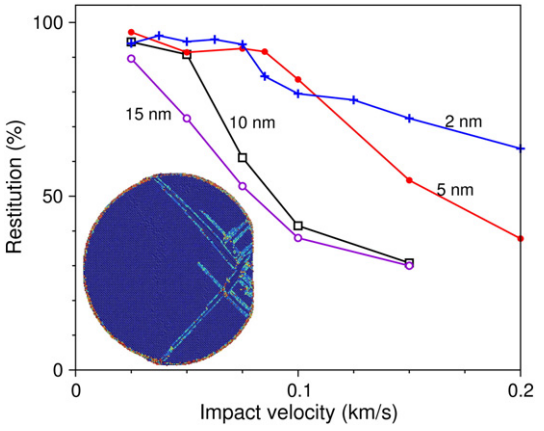

Fig. 3. Velocity restitution vs. impact velocity for different particle sizes. Inset: a cross-section of the atomic configuration for $r = 15$ nm, $v_i = 0.15$ km s^{-1} and $t = 20$ ps. Color-coding is based on central symmetry, with fcc, hcp and non-close-packed atoms denoted approximately with blue, light blue and red, respectively.

$R>0.9$), and the non-close-packed atoms may appear without the hcp atoms; their numbers increase with decreasing R. R is well correlated to and explained with the degree of plastic deformation and heating (see below). For example, an increase in the peak percentage of the hcp atoms from 2% to 8% translates to a decrease in R from about 0.4 to 0.3 (Figs. 1(b) and 3; $r=10$ nm). An observation of particular interest is that the impact-induced structure changes (e.g., stacking fault-related dislocations) can be highly transient and reversible largely due to the size and short time scales involved in the impact. As illustrated in Fig. 1(b) for $r=10$ nm ($v_i=0.1$ and 0.15 km s^{-1}), the fcc–hcp structure change is nearly completely reversed for the former (with minor remnant of non-close-packed atoms, ~0.1%), while it is relatively stable (though reduced) for the latter. This structural reversal also occurs at $v_i \lesssim 0.15$ km s^{-1} for all sizes except $r=15$ nm ($\lesssim 0.075$ km s^{-1}), and the run-to-run fluctuations exist for $r=1$ and 2 nm.

The total energy of the whole system consists of the kinetic energy related to the center of mass (E_c) and internal energy (E), and is conserved regardless of the particle size and impact velocity. The energy loss in E_c is $\frac{1}{2}m(v_i^2-v_t^2)$ before and after impact (m denotes mass). ΔE (the change in internal energy) is related to temperature changes, and work related to volume and surface-area variations. Energy can flow either way between E and E_c. The smallest particles ($r=1$ nm) are more susceptible to random fluctuations because of their high surface-area-to-volume ratio. As a result, E can be converted into E_c (ultra-elastic impact) or vice versa (inelastic impact). For example, a loss of 32 μeV per atom in E to E_c induces about 7% ultra-elasticity of impact for $v_i=0.025$ km s^{-1} (Fig. 2(b)), despite a very slight increase in T; and the total energy is conserved. For larger cluster sizes (≥ 2 nm), E_c is lost to E, and $\Delta E=-\Delta E_c \approx C_v \Delta T$ since the volume and surface area undergo small or negligible changes. Here C_v is the specific heat at constant volume, and is about $3R$ with R being the gas constant. In the case of $r=10$ nm and $v_i=0.1$ km s^{-1}, ΔT is about 10 K as directly obtained from the MD simulations (Fig. 1(c)), in accord with the estimation from $|\Delta E_c| = C_v \Delta T$ (about 10.6 K). Note that the fcc–hcp structure change is transient and reversible in this case (Fig. 1(b)), and it still induces a noticeable temperature rise. In the case of $r=10$ nm and $v_i=0.15$ km s^{-1}, the fcc–hcp change is only partially reversed (Fig. 1(b)) and heating is more pronounced ($\Delta T \sim 23$ K; Fig. 1(c)). This irreversible heating leads to reduced velocity restitution. Thus, the fcc–hcp structure change causes irreversible energy dissipation, regardless of its reversibility. ΔT is trivial at low v_i (perfectly or highly elastic impact) and increases with the degree of the fcc–hcp transition, ranging from about 0 K to 25 K in all the cases examined. (Inelastic impact may occur even without plasticity in the final structure due to heating or fluctuations during impact.) For comparison, the impact heating of Si nanospheres was related to phase-transition plasticity [6].

The stress field within the nanoparticle during impact is three dimensional for current impact geometry; it is more complex than the geometry with spherical or planar symmetry [1]. Shown in Fig. 4 are examples of the stress profile (σ_{xx}) for two different sizes ($r=5$ nm and 10 nm) at the same v_i (0.1 km s^{-1}). Although the peak values are similar as expected, the stresses are more sustained in space and time (not shown) for larger sizes, leading to more pronounced plasticity/heating and thus less velocity restitution. (This can also be seen from the differences in Δt_{sp}, e.g., it is about 15 ps and 30 ps for the two cases shown in Fig. 4, respectively.) The size effect may become less pronounced when v_i is sufficiently large (e.g., 0.15 km s^{-1} for $r=10$ and 15 nm, Fig. 3), since plasticity/heating depends both on velocity and size.

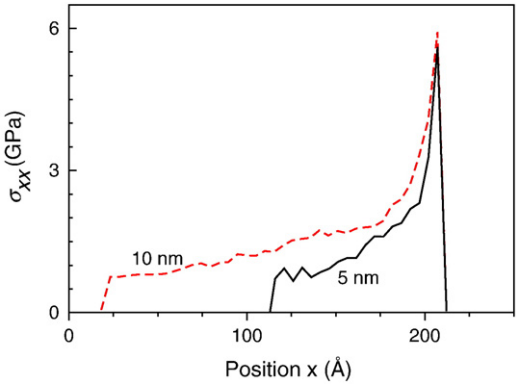

Fig. 4. The stress profile snapshots (maximum in time) for impact at $v_i=0.1$ km s^{-1}.

4. Conclusion

The impact of small nanoparticles ($r\sim 1$ nm) with a rigid wall can be ultra-elastic or inelastic soly due to fluctuations, and the impact can still be highly elastic at larger sizes (about 2–15 nm). The reduced velocity restitution is mostly due to reversible or irreversible fcc–hcp transitions induced by impact, which in turn gives rise to irreversible heating. Inelastic impact may occur without remnant plasticity. Increasing impact velocity and particle size normally increases plastic deformation and thus impact inelasticity.

Acknowledgement

L.B.H. acknowledges the support from NSFC Grant Nos. 40574043 and 40537033. This work is a part of the PSAAP project funded by the U.S. DOE contract DE-FC52-08NA28613 under grant DMR-0520547. S. N.L. is grateful for the support from a DOE Energy Frontier Research Center: Materials at Irradiation and Mechanical Extremes. LANL is under the auspices of U.S. DOE under contract No. DE-AC52-06NA25396.

References

[1] Kanel GI, Razorenov SV, Fortov VE. Shock-wave Phenomena and the Properties of Condensed Matter. New York: Springer; 2004.
[2] [2] W. Goldsmith, *Impact* (Dover, 2001).
[3] Järvi TT, Pakarinen JA, Kuronen A, Nordlund K. Eur Phys Lett 2008;82:26002.
[4] Brilliantov NV, Spahn F, Hertzsch J-M, Pöschel T. Phys Rev E 1996;53:5382.
[5] Kuninaka H, Hayakawa H. Phys Rev E 2009;79:031309.
[6] Suri M, Dumitrica T. Phys Rev B 2008;78:081405.
[7] Bridges FG, Hatzes A, Lin DNC. Nature 1984;309:333.
[8] Tomsic A, Schröder H, Kompa KL, Gebhardt CR. J Chem Phys 2003;119:6314.
[9] Kalweit M, Drikakis D. Phys Rev B 2006;74:235415.
[10] Rogan J, Ramirez R, Romero AH, Kiwi M. Eur Phys J D 2004;28:219.
[11] Mishin Y, Mehl MJ, Papaconstantopoulos DA, Voter AF, Kress JD. Phys Rev B 2001;63:224106.
[12] Luo SN, Han L-B, Xie Y, Zheng LQ, Xia K. J Appl Phys 2008;103:093530.
[13] Honeycutt JD, Andersen HC. J Phys Chem 1987;91:4950.
[14] Kelchner CL, Plimpton SJ, Hamilton JC. Phys Rev B 1998;58:11085.
[15] Li J. Modell Simul Mater Sci Eng 2003;11:173.